

Evaluation of Biocompatibility of Chitosan Films from the Mycelium of *Aspergillus niger* in Connective Tissue of *Rattus norvegicus*

Danny Javier Balanta Silva¹, Fabio Zuluaga^{1*} and Carlos H²

¹Departamento de Química, Universidad del Valle. Cali, Colombia

²Escuela de Odontología, Universidad del Valle. Cali, Colombia

*Corresponding author: Fabio Zuluaga, Departamento de Química, Universidad del Valle. Cali, Colombia, E-mail: hector.zuluaga@correounivalle.edu.co

Received date: May 29, 2015; Accepted date: July 20, 2015; Published date: July 27, 2015

Copyright: © 2015 Silva DJB, et al. This is an open-access article distributed under the terms of the Creative Commons Attribution License, which permits unrestricted use, distribution, and reproduction in any medium, provided the original author and source are credited.

Abstract

Chitosan was extracted from *Aspergillus niger* mycelium and characterized by several techniques (FTIR, ¹H-NMR y ¹³C-CP-MAS-NMR, TGA, DSC and XRD) with a reaction yield of 5.02%, and its average viscosity molecular weight was 1.52 x 10⁵ g/mol. Deacetylation degree was determined by elemental analysis and ¹H-NMR, being around 75%. Chitosan films were obtained by film casting, using glycerol and oleic acid as plasticizers, the chitosan films were characterized by SEM and XRD. Degradability *in vitro* tests under physiological conditions, mechanical tests, and biocompatibility tests on *Rattus norvegicus* were run, followed by histological studies of connective tissue samples from the site where the films were implanted finding complete absorption of the material and no damage to nearby tissues.

Keywords: Tissue engineering; Chitosan films; Biocompatibility, *In vivo* and *in vitro* degradability

Introduction

Polymeric devices are used to study tissue and organ regeneration as well as their function [1]. Chitin is a natural polymer present in crustacean shells and some fungi cell walls which, under hydrolysis, yields its deacetylated analogue chitosan. The mycelia of various fungi such as *Absidia coerulea*, *Absidia glauca*, *Aspergillus niger*, *Gongronella butleri*, *Mucor rouxii* and *Rhizopus oryzae*, among others, have been suggested as alternative chitosan sources [2-6]. In the production of citric acid by a local industry, 13500 ton/year of *Aspergillus niger* mycelium are left that can be a chitosan cheap source as only 10% is used for animal food supplement and agricultural fertilizer.

Crustacean shells availability is uncertain as their exploitation is limited to certain months of the year therefore fungal chitosan was chosen as the raw material for the extraction of chitin and its conversion to chitosan. Some other reasons for this choice are a more time consuming chitin extraction process from crustacean which involves additional steps (demineralization with hydrochloric acid and deproteinization) [7], and the possible presence of allergenic components [8].

In contrast, chitosan extraction from fungi requires fewer isolation steps (deacetylation of chitin, extraction of chitosan in acidic medium, precipitation in alkaline medium), and leads to an allergen-free product, also, *Aspergillus niger* mycelium is an available source for chitosan isolation throughout the year [9].

Chitosan is a soluble polymer in aqueous acidic solutions and the extent of its solubility depends on the following properties: deacetylation degree (DD), viscosity, and average molecular weight. A high DD and a low to medium molecular weight increase the solubility [10-12]. On the other hand, this polymer is well known for its degradability, biocompatibility, and a wide variety of applications that

have been found in different fields: agriculture, pharmaceutical and food industry and medicine [2], including the production of scaffolds for tissue regeneration [13,14].

As a versatile polymer, chitosan can be processed in different ways: films, fibers, spheres and porous structures allowing its use in tissue regeneration, such as conveyor cells, bioactive substances, and drug release. Also, chitosan can work alone or in combination with other materials like PLA (poly-L-lactic acid) [8,15-17].

The present study presents the use of chitosan as a scaffold for tissue regeneration.

Experimental

Materials and reagents

Acetic acid (JT Baker, 99.90%), oleic acid (Merck, 99%), potassium chloride (Merck, 99.50%), sodium chloride (Merck, 99.5%), ethanol (Sigma-Aldrich, 99.80%), monobasic potassium phosphate (Merck, 99%), dibasic potassium phosphate (Merck, 98%) potassium hydrogen phthalate (Merck, 99%), Glycerin USP (Agenquímicos, 99.71%), partially dried *Aspergillus niger* fungal mycelium (10% moisture, Sucroal S.A, 99%) sodium hydroxyde analytical grade (NaOH, 99%, Merck), commercial chitosan for comparisson (Sigma-Aldrich, 150000-310000 Da, 75-85 deacetylated). All reagents were used as received.

Chitosan extraction from *Aspergillus niger*

Extraction of chitosan was carried out by the same method previously employed in our laboratories [18].

Physicochemical chitosan characterization

Spectroscopic characterization of chitosan: Chitosan and chitosan films were characterized by infrared spectroscopy, using an IR

ThermoScientific Nicolet 6700 spectrophotometer (KBr disc) with a resolution of 2 cm^{-1} 16K scans and recorded between $4000\text{-}500\text{ cm}^{-1}$. The $^1\text{H-NMR}$ spectra of chitosan were read on a Bruker Avance II UltraShield 400 MHz NMR spectrophotometer, using a solvent mixture composed by CF_3COOH (two drops) and DMSO-d_6 as deuterated solvent, at a temperature of 25°C . Chitosan were also characterized by solid $^{13}\text{C-NMR}$ CP-MAS (Cross Polarized Magic Angle Spinning) at the following conditions: 5 mm diameter zirconium rotor at a 100 MHz frequency, 653 scans for reading, sweep frequency of 29760 Hz, acquisition time of 1.10s at a temperature of 25°C .

Deacetylation degree and determination of molecular weight: Deacetylation Degree (%DD) was determined for chitosan by triplicate, using an elemental analyzer Thermo Flash EA 1112 series. DD was calculated through C/N ratio of the N-acetylated chitosan units, according to Equation 1 [19].

$$\%DD = 100 - \left(\frac{\frac{C}{N} - 5.145}{1.716} \right) * 100 \text{-----(1)}$$

Deacetylation degree also was determined by nuclear magnetic resonance $^1\text{H-NMR}$, given the relative integrals of the signals of the acetic acid and N-acetyl chitosan methyl groups appearing between 1.8-2.1 ppm and H2-H6 hydrogens in region between 2.7-4.4 ppm, according to equation 2 [20,21].

$$\%DD = \left[1 - \left(\frac{\frac{1}{3}HAc}{\frac{1}{6}H2-H6} \right) \right] * 100 \text{-----(2)}$$

Determination of average molecular weight of chitosan (M_v) was performed by capillary viscometry using chitosan solutions with concentrations from 0.0001 to 0.001 g/mL dissolved in a 1:1 mixture of 0.1 M acetic acid and 0.2 M NaCl, leaving immersed Ubbelohde # 0B-206 in a thermostatic bath Lauda Alpha RA 8 to 25°C , following previously methodologies [10,22] and the obtained data were analyzed using the Huggins and Mark-Houwink-Sakurada equations [19].

Thermal analysis of chitosan: Thermal stability of chitosan was determined on a TA Instruments 2050 thermobalance adjusted in a temperature range between 25 to 300°C , under a continuous nitrogen gas flow of 50.0 mL/min. Glass transition temperature (T_g) was determined using a differential scanning calorimeter DSC-Q100 in a temperature range between -89 to 320°C . Both analyses were performed at a heating rate of $10^\circ\text{C}/\text{min}$.

X-ray diffraction (XRD) and scanning electron microscopy (SEM): X-ray diffractograms of chitosan films were taken in a PANalytical X'Pert Pro powder diffractometer using a copper tube ($\text{CuK}\alpha 1$) of 320 mm in diameter, at a wavelength of 1.5405 \AA , 45 kV and 40 mA. The samples were read in a 2θ working range between 5 to 120° with 2000-6000 scans.

Morphology of the films was studied by scanning electron microscope (SEM) using a JEOL JSM-6490LV scanning microscope using secondary electron irradiation at 20 kV, with 200x magnification and a 10-100 μm scale.

In vitro test and mechanical test: *In vitro* degradation was performed according to ASTM F1635-11 [23] simulating physiological conditions (T : 37°C , pH : 7.47) using a buffer solution prepared mixing NaCl (137 mM), KCl (2.68 mM), K_2HPO_4 (10.14 mM) and KH_2PO_4

(1.76 mM). Weight changes were tracked every 3 days over a period of seven weeks. Mechanical testing of the films was conducted according to ASTM D638 [24] standard in the HK50S Tinius Olsen Universal Testing machine applying a pulling speed of 5 mm/min.

Preparation of chitosan film

Chitosan films were prepared using the film casting method (solvent evaporation) [25,26] mixing the polymer in 1% acetic acid (w/v) solution with the plasticizer mixture (1:1 glycerol and oleic acid both 1%, respectively). The ratios between polymer and plasticizer mixture in the films were varied from 50:50; 60:40; 70:30; 80:20; 90:10 to 100: 0 (no plasticizer). Each mixture was subjected to mechanical stirring for 2h at 25°C at a speed of 150 rpm. After shaking, solutions were placed in Petri polyethylene dishes and allow to dry in an oven at 60°C for 48 h until obtain constant weight.

In vivo biocompatibility studies and histological studies

Subcutaneous implantation of chitosan films was performed in five male Wistar® lab rats (*Rattus norvegicus*), with weights between 180-200 g. Five lab rats were chosen to be implanted in this study, kept in individual cages in an animal facility, checking daily feeding rate, temperature and body weight, under constant monitoring, following the guidelines of ISO 10993-6 8.5.3 (Animals and Implantation) standard [27].

Pre surgical procedure: In each animal a mixture of sedatives acepromazine maleate (0.6 mg/kg, intramuscular); 2% xylazine (0.6 mg/kg, intramuscular) and ketamine (0.7 mg/kg, intramuscular) were used. Subsequently it was determined that the material would be implanted in subdermal way for a period of 21 days.

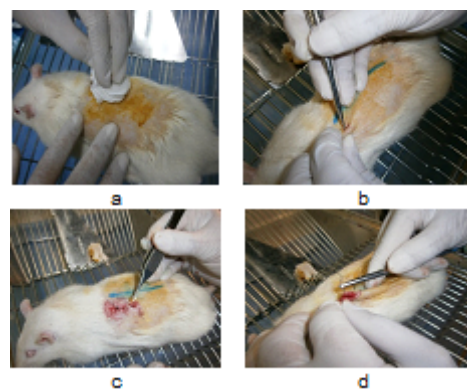


Figure 1: Process of implementation of the chitosan films: shaving and disinfection (a); incision in the epidermis (b); implantation of the films (c); suturing of the dorsal area (d).

Surgical procedure: The dorsal region of each one of the animal biomodels were disinfected using Isodine® (povidone iodine) (Figure 1a), after that, 2 cm length incision was made in the dorsal midline with handle scalpel blade # 3 and # 15 up to the subcutaneous tissue (Figure 1b). Using blunt forceps three subcutaneous pockets were created on each side of the midline (Figure 1c) and three 6 mm diameter chitosan films discs were implanted in the left thoracic region, and in the right dorsal region, commercial chitosan 6 mm diameter discs were implanted as control. The surgical incision was

closed with simple absorbable suture and topical gentamicin was applied to protect the sutured area (Figure 1d). In post-operative cares clindamycin (600 mg/Kg, intramuscular) and tramadol (2 mg/kg, intramuscular) was applied. Finally in the next five days after the implantation, acetaminophen (100 mg/Kg) was used for pain and inflammation.

Euthanasia and retrieval of samples: after 21 days, the biomodels were euthanized using Eutanex® (390 mg pentobarbital sodium and phenytoin sodium 50 mg, 0.04 mL/kg, intraperitoneal). Samples for histological analysis were retrieved from the surrounding connective tissue implantation, and were fixed in a buffer solution of phenol, 10 mM TRIS HCl and 1 mM EDTA at pH 8.0, through paraffin embedding method. Hematoxylin and eosin staining were used as cellular staining/revealing agents.

Results and Discussion

Fungal cell wall hydrolysis and chitosan isolation

During hydrolysis under alkaline medium the *Aspergillus niger* cell wall breaks down, releasing the internal components, some of them being: proteins, carbohydrates and sugars, and finally chitin-glucan complex. Under the pH change, proteins in the cell wall get denatured, resulting in the formation of soft slurry. In the case of carbohydrates and sugars, the temperature rise caused their degradation and as a result, the soft paste acquired a brown color. Degraded sugars could be separated completely from the slurry through successive washes with water, leaving a brown alkaline pH effluent, and leaving untouched the chitin glucan complex (insoluble in water, in a 27.1215g dry basis).

Due to alkaline hydrolysis of the glycosidic linkages, the chitin-glucan complex is separated into two different polysaccharides: chitin and glucans.

With isolated chitin, basic hydrolysis occurred at the chitin N-acetamido groups (deacetylation) at the specified reaction conditions (40% NaOH, time of 4h, and a high temperature, 110°C) releasing the chitosan (with acetylated and deacetylated units along the polymer chain).

Chitosan (insoluble in water and at alkaline pH) remains in the soft slurry mixed with glucans. To separate it, was necessary to decrease the pH using acetic acid to a range of 3.4-3.8, solubilizing the free amino groups of the chitosan, allowing it to be soluble in aqueous solution. One advantage of using acetic acid is the procedure at room temperature without further heating, to solubilize the chitosan unlike, for example, the use of HCl [28].

The complete separation of the solubilized chitosan occurs through mechanical separation methods such centrifugation and filtration. When centrifuge is used, the polymer remains in the supernatant phase and the denser components (water-insoluble glucans in the slurry) remains at the bottom of the containers.

Finally, the soluble chitosan is separated from the aqueous solution by precipitation after dropwise addition of NaOH 30% w/v, reaching a pH between 9-11, considering that chitosan exhibits usual behavior of a primary amine in an acid base equilibrium.

Regarding the reaction yield (5.02%) it should be noticed that it depends on several factors: the fungal strain to be used, type of fermentation (continuous or batch), composition of the fermentation medium and culture conditions fermentation (inoculum size, time and

temperature of fermentation) and extraction procedure [29], being this fungal extraction procedure able to show yield percentages between 1.2 to 10.4% for different fungal chitin containing species [3,4,30,31], so the value obtained here is comparable to previous studies [32-34].

Infrared spectroscopy (FTIR) and nuclear magnetic resonance (NMR) of extracted chitosan

Figure 2 shows the infrared spectrum of isolated chitosan. The stretching vibration of the amino group (ν NH) appears at 3445 cm^{-1} connected to the stretching vibrations provided by the hydroxyl groups (ν OH). Next, at 2927 cm^{-1} appears symmetric stretching vibration of the carbon – hydrogen bond (ν s CH), then at 1663 cm^{-1} is found stretching vibration of the carbonyl group (ν C=O, type I amide band), while the deformation vibration (ν NH, type II amide band) appears at 1549 cm^{-1} . Deformation vibration of the methylene groups scissors (δ s CH) appears at 1426 cm^{-1} , the stretching vibration of the bond (ν CN, type III amide band) is seen at 1320 cm^{-1} , then at 1171 cm^{-1} , the stretching vibration of C-O single bond (ν CO) appears. Finally, the bands at 1078 and 895 cm^{-1} shows the β -(1,4) bonds in chitosan, corresponding to C-O-C glycosidic linkage bonds. The assigned infrared bands are similar to those already reported previously in the literature [35,36].

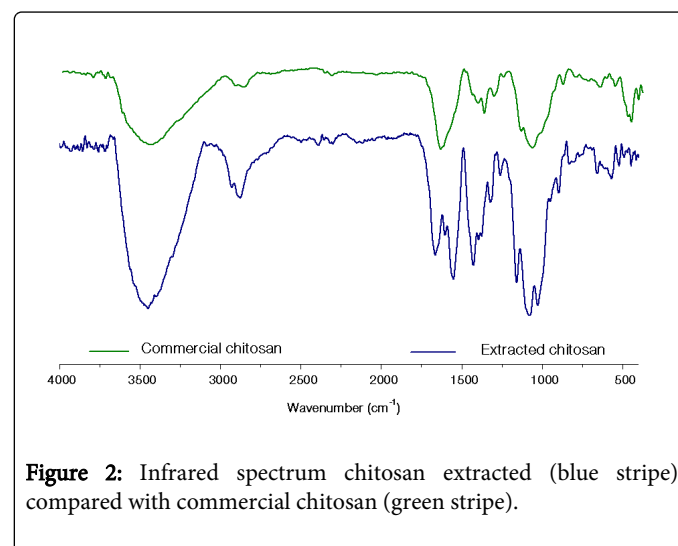


Figure 2: Infrared spectrum chitosan extracted (blue stripe) compared with commercial chitosan (green stripe).

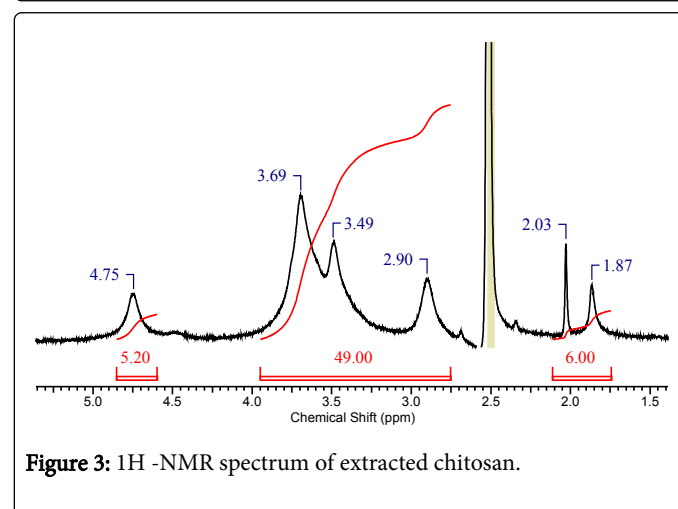


Figure 3: 1H -NMR spectrum of extracted chitosan.

In the ¹H NMR spectrum, the 1.87 ppm chemical shift appears as a singlet for the hydrogens of methyl group of the acetic acid, at 2.03 ppm appears as a singlet for the methyl group hydrogens related to the acetamido group (NHCOCH₃) in N-acetyl-D-glucosamine, at 2.90 ppm appears the H2 proton signal of the D-glucosamine, after that, the region located between 3.49-3.69 ppm shown a broad signal that keeps together H3-H6 protons units of D- glucosamine and N-acetyl-D-glucosamine fractions, at 3.69 ppm, appears the corresponding signal to the hydrogens of the amino group signal, superimposed with the previously mentioned signals, and at 4.75 ppm appears the H1 proton signal corresponding to the D-glucosamine hydrogens. For clarity reasons, the signal of the solvent employed (DMSO-d₆) appears highlighted at 2.53 ppm (Figure 3).

The solid state ¹³C-NMR CP-MAS spectrum (Figure 4) shows at 28.22 ppm the corresponding signal to the methyl group in acetamido moiety; C2 ring signal appears belonging to 62.16 ppm; the signal at 65.58 ppm is related to C6 in the ring, the C3 and C5 ring signals appears at 79.89 ppm, now, the C4 ring signal appears on 87.89 ppm; then, the C1 ring signal appears to 109.91 ppm, and finally the carbonyl group (C=O) signal belongs to the acetamido moiety showing little intensity in 179.24 ppm. It is concluded that assigned signals match those previously reported [7,20,35].

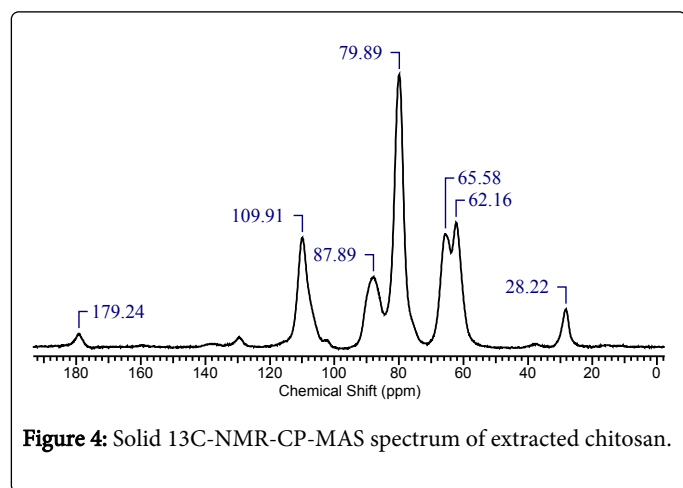


Figure 4: Solid ¹³C-NMR-CP-MAS spectrum of extracted chitosan.

Deacetylation degree and average molecular weight for extracted chitosan

According to the values shown by elemental analysis, we found that carbon content in the sample corresponds to 38.23% ± 0.48% hydrogen content corresponds to 6.79 ± 0.18%, and nitrogen content corresponds to 6.84 ± 0.02. Using equation 1, the degree of deacetylation by elemental analysis (%DD) for the extracted chitosan leads to 74.15%, a consistent value that highlight the solubility of the polymer, since over than 70% of the amino groups (NH₂) in the polymer chain are available for being protonated.

Using equation 2, and the ratio of relative integrals area of the ¹H NMR spectrum of Figure 3, we found that the degree of deacetylation (%DD) of the chitosan is 75.51%, which is very close to the determined by elemental analysis, and closer to previously reported values [9,33,34].

Average molecular weight of chitosan was found through Huggins equation (Equation 3), processing the data in order to obtain a linear

relationship, being the plot intercept referred to intrinsic viscosity (119.06 mL/g). means reduced viscosity, and KH is the Huggins constant obtained experimentally in this process from the slope of the linear plot (not shown), and is the concentration of each chitosan diluted solution.

$$\frac{\eta_{sp}}{c} = K_H[\eta]^2 \rho_b + [\eta] \text{-----(3)}$$

$$M_v = \left(\frac{[\eta]}{K} \right)^{1/\alpha} \text{-----(4)}$$

The intrinsic viscosity value is replaced in Mark-Houwink-Sakurada equation (Equation 4) along with the empirical constants for the polymer-solvent system described in the experimental section, corresponding to K=1.81 × 10⁻³ mL/g and α=0.93 gathered from previous reports [10,22]. Therefore, the average molecular weight of chitosan (M_v) corresponds to 1.52 × 10⁵ g/mol, fitting in the range (1 × 10⁵-5 × 10⁵ g/mol), usable for biomedical applications according to literature [37].

Thermogravimetric (TGA) and differential scanning calorimetry (DSC) experiments for chitosan

The thermogram of chitosan (Figure 5) indicates different weight losses. The first heat loss event was due to the presence of water bound to chitosan by hydrogen bonds (42.16°C, 0.95% and 132.09°C, 9.97%), the following events thermal losses (213.88°C, 13.47%, 265.16°C, 28.32%) are related to the cleavage of O-glycoside bonds and attributed to degradation of chitosan chains, leaving off oligomers. Finally at 299.23°C, chitosan has lost 44.61% of its original weight, being relatively stable at that temperature [38].

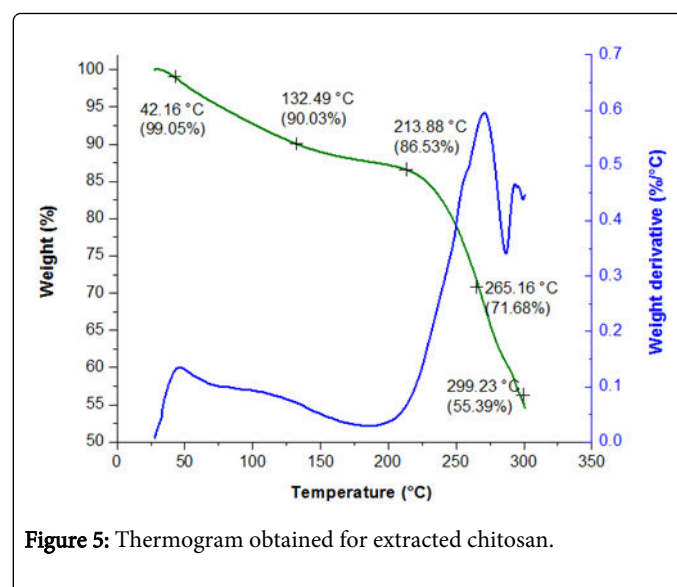


Figure 5: Thermogram obtained for extracted chitosan.

According to differential scanning calorimetry (DSC) plot, the glass transition temperature (T_g) found for chitosan was 124.36°C, and the decomposition temperature of the polymer occurs at 288.77°C, being

these observations of a chitosan when the degree of deacetylation (DD %) is around 70-80% [37] (Figure 6).

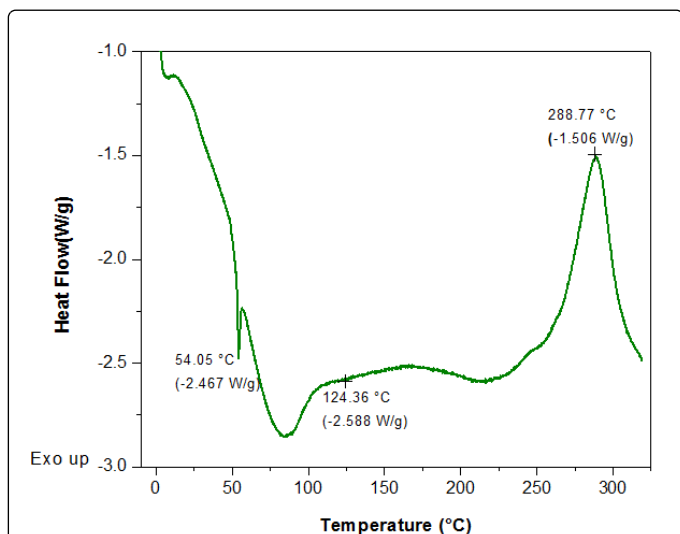


Figure 6: Differential scanning calorimetry for extracted chitosan

X-ray diffraction (XRD)

Three crystalline reflections were seen in the range of 5-40°, reported in the literature as 020 (9.51°), 110 (19.78°), and 120 (26.30°) [28,39], being an amorphous material chitosan since the conformation of the polymer chains corresponds to α -chitin, characteristic of the source: cell wall of fungi. If chitin chains were from β -chitin, 020 reflection will not appear. XRD of the chitosan films appear the same as chitosan, the difference is a slightly displaced crystalline reflections (13,16 and 25°) due to the presence of oleic acid and glycerol as plasticizers.

Hydrolytic degradation test and mechanical test

The tensile strength and length of the pristine chitosan film (without plasticizer) correspond to 30.06 MPa and 16.7 mm, it is expected that the addition of plasticizer mixture (glycerol and oleic acid) helps to decrease the initial tensile strength and increase the initial length parameter, as happened in the 80:20 chitosan film (25.50 MPa, 20.6 mm) and 90:10 chitosan film (27.90 MPa, 25.6 mm) respectively, due to the loss of stiffness of chitosan chains with an increased flexibility provided by the plasticizer.

Given the above, the trend was not the same in 50:50 (26 MPa, 3 mm), 60:40 (12 MPa, 5 mm) and 70:30 (9 MPa, 6 mm) chitosan films, because although they exhibited decrease in the tensile strength, they showed no increase in length due to the excessive separation of chitosan chains by action of the plasticizer [40,41] (Figure 7).

In vitro test of chitosan films with plasticizer mixture under simulated physiological conditions (Figure 8) shows 6-15% remaining material at half time of the study (3.5 week), and 2-9% of remaining material after the seventh week.

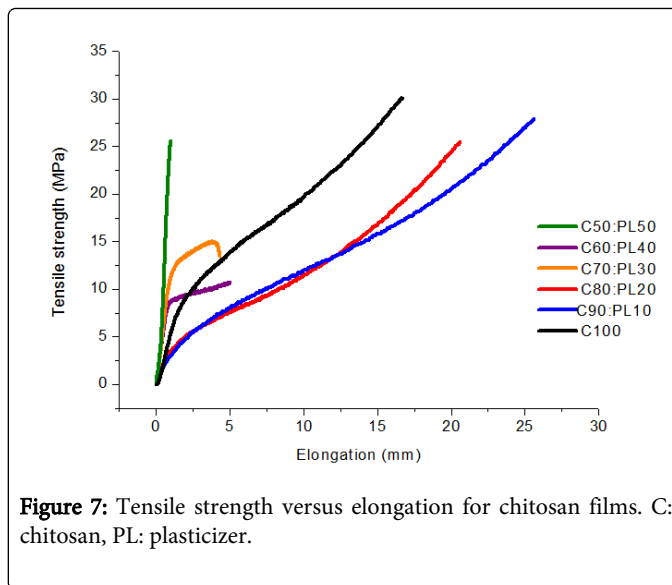


Figure 7: Tensile strength versus elongation for chitosan films. C: chitosan, PL: plasticizer.

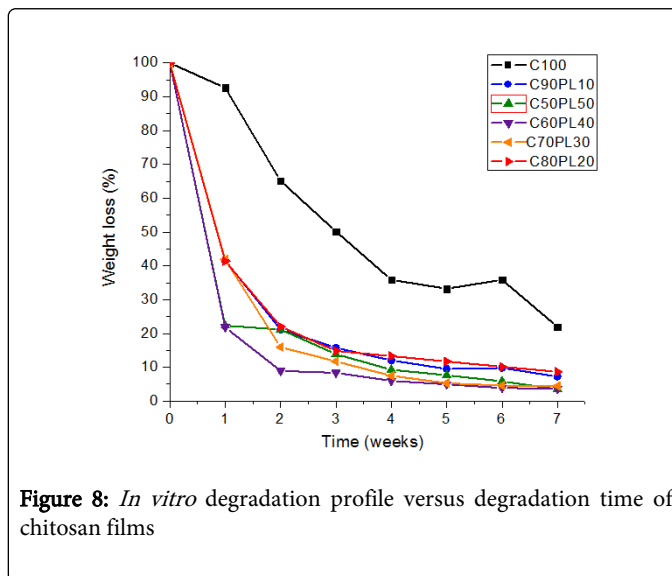


Figure 8: *In vitro* degradation profile versus degradation time of chitosan films

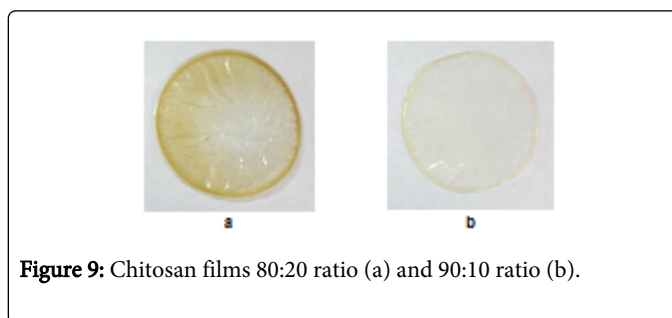


Figure 9: Chitosan films 80:20 ratio (a) and 90:10 ratio (b).

The quick degradation of chitosan films containing plasticizer compared to pristine chitosan film (without plasticizer) is due to the increased flexibility of chitosan chains as the addition of glycerol reduces stiffness and increases the separation between the polymer chains, consistent with the decrease in tensile strength parameters and the increase in elongation or extension discussed above, but in the case of 50:50, 60:40 and 70:30 (polymer: plasticizer ratio) chitosan films, the excessive amount of plasticizer shows a disadvantage for the three

cases, because tensile strength and elongation parameter are lower compared to pristine chitosan film. Therefore, chitosan films of 80:20 and 90:10 ratios were suitable for implantation purposes [6] (Figure 9).

Scanning electron microscopy for chitosan films

Both chitosan films show common elements in morphology, particularly porosity and uniformity: 80:20 film (Figure 10a) at a 200× zoom, pores were achieved and its size in the micrometer range, allowing cells to grow and build new tissues. The micrograph in Figure 10b corresponding to the 90:10 film indicates a 200× zoom continuity across its surface; small pores can be seen, and a bump caused during evaporation of the solvents that indicates a non-completely smooth homogeneous surface, without affecting the quality of the material.

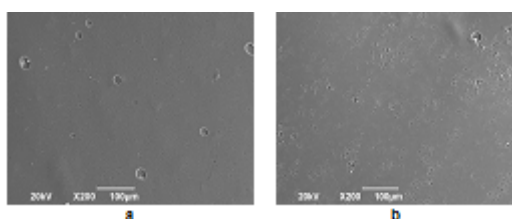


Figure 10: Scanning Electronic Microscopy for 80:20 chitosan film (a) and 90:10 chitosan film (b).

In general, we can say that thanks to the porous zones exhibited by the films, the delivery of oxygen, nutrients and cell growth transport can occur, making cell replication easier [42], because chitosan is a polymer with a high affinity for extracellular matrix elements [43].

Even if the device had not shown a porous form, the pores can be formed in situ once the material is implanted, functioning as a scaffold, suitable for the final application. These two situations are presented in the prepared films. Adding to the above, the pore size on the films ranged from 1-100 micrometers in 80:20 and 90:10 chitosan films, making the synthesized material in the laboratory suitable for its use as scaffolding platforms, comparable to similar chitosan scaffolds (extracted from the fungus *Gongronella butleri* (average molecular weight of 5×10^4 g/mol and a 77% deacetylation degree, combined with human fibroblasts, which had a porosity between 60 to 90 micrometers leading a material with average pore size of 84 micrometers) [44].

It should be pointed out that pore size is a useful parameter for tissue regeneration: if the tissue is soft type (skin, for example), the average pore size should be 40-140 micrometers for adequate cell growth, [45] and in rigid tissues (such as bone), the scaffold should have a mean pore size of 100-135 micrometers to induce bone growth, with a preferred upper size 300 micrometers for vascularization and bone formation [46].

Histological studies in animal biomodels

The potential application of a material in tissue regeneration will depend on their behavior in three aspects: viability, migration, proliferation and cellular differentiation, which are key elements in cell-biomaterial interaction. Viability refers to biocompatibility and biodegradation/bioresorption, which are basic characteristics required for an element to be used as matrix, since the material must be placed

in situ, be degraded or resorbed at a particular time, allowing the absorption of plasma proteins and specific binding to cells according to their final application. For that reason a chitosan implantation period of 21 days was chosen, a suitable time to allow cell and new tissue growing (Figure 11). Migration, proliferation and cell differentiation are generic process not specific to chitosan, and it is well known that chitosan can act as a chemotactic and an attractant agent for neutrophils [47,48].

Different studies show that chitosan is biocompatible both *in vitro* and *in vivo* conditions, and it promotes cell chemotaxis involved in the first stage of the inflammatory response, besides allowing the growth, proliferation and differentiation qualities that make it ideal for use in tissue regeneration techniques [49-51]. Samples were completely absorbed in the five animal biomodels without leaving traces of implanted material; the macroscopic appearance of the dermis looks completely healthy without signs of inflammation or foreign body enclosement indicating biocompatibility as expected.



Figure 11: Incision in the dorsal region (a) and verification of the absorption of the samples (b) after 21 days of implantation.

Figure 12 shows the histological micrographs for the first and third animal respectively (for the other animals the same situation was observed) using hematoxylin and eosin to distinguish different tissues. The first animal biomodel micrograph shows the connective tissue (light pink) with normal, hair follicles (elongated ovals) and sebaceous glands (small white balls), the deep dermis adipocytes (thick white line), and muscle tissue (pink granules) are normal, without evidence of foreign bodies or remains of implanted polymeric material (Figure 12a).



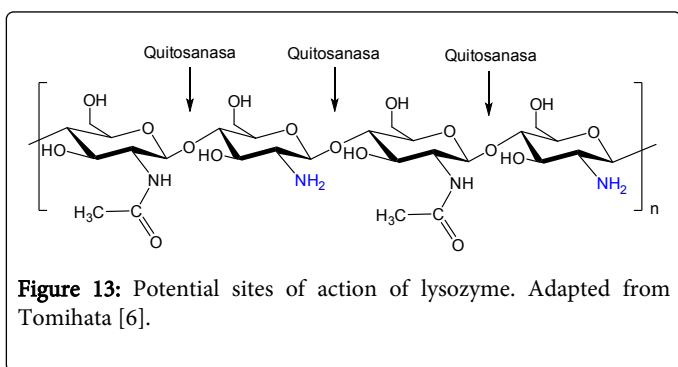
Figure 12: Histological micrographs for animal biomodel 1 (a) and animal biomodel 3 (b).

The third animal biomodel also evidenced the discussed above (mostly healthy tissue) with the difference of some remaining pieces of the implanted polymeric material film being surrounded by connective tissue, also the remaining part shows white gaps at the middle of Figure 12b, demonstrating the degradation to oligosaccharides or glycosaminoglycans.

Finally, although chitosan was biocompatible and harmless after implantation, is not a naturally occurring compound in the body of

the animal biomodels studied. As a result, it is likely to be degraded or metabolized by action of macrophages and phagocytes, into products present in the extracellular matrix such as glycosaminoglycans, D-glucosamine and N-acetyl-D-glucosamine [6,52].

One possible chitosan *in vivo* degradation in animal biomodels occurs by enzyme release, such as lysozyme, capable of breaking the $\beta(1,4)$ linkages between chitosan chains, transforming them into oligosaccharides and D-glucosamine monomers [6], that can be recycled by the organism and excreted later [53]. Figure 13 shows potential cleavage/breaking sites in O-glucoside bonds in chitosan by the enzyme lysozyme, releasing by-products described above.



In addition, physiological fluids released in animal biomodels could degrade the films (being recognized as foreign bodies), minimizing its presence into the body due to hydrolysis or pH changes [54].

Conclusion

Extraction, identification and physicochemical characterization of chitosan from the mycelium of *Aspergillus niger* was achieved. Chitosan films exhibited suitable morphology, having acceptable mechanical properties and were degraded under simulated physiological conditions over a period of seven weeks, making them suitable for implantation. *In vivo* studies show that implanted chitosan films were biocompatible and absorbable, and were not found within the biomodels, not affecting connective tissue and its surroundings after the implantation period, leaving the tissue healthy.

The biocompatibility and bioabsorption characteristics shown by the films may allow their use for wound healing and as occlusive barrier in guided tissue regeneration techniques.

Acknowledgements

The authors thank the Universidad del Valle (SIMERQO research group and Medical dental school) for financial support and infrastructure used in this project. We also thank the center of excellence for new materials (CENM) for the donation of some reagents, and finally Sucroal S.A. for the donation of mycelium.

References

1. Meyer U, Meyer T, Handschel J, Wiesmann H (2009) Fundamentals of Tissue Engineering and Regenerative Medicine. Springerli, Springer Berlin Heidelberg: Berlin, Heidelberg.
2. Rinaudo M (2006) Chitin and chitosan: Properties and applications. Prog Polym Sci 31: 603–632.
3. Synowiecki J, Ali N, Quawi A (1997) Mycelia of *Mucor rouxii* as a source of chitin and chitosan. Food Chem 60: 605–610.
4. Rungsardthong V, Wongvuttanakul N, Kongpien N, Chotiwaranon P (2006) Application of fungal chitosan for clarification of apple juice. Process Biochem 41: 589–593.
5. Pochanavanich P, Suntornsuk W (2002) Fungal chitosan production and its characterization. Lett Appl Microbiol 35: 17–21.
6. Tomihata K, Ikada Y (1997) In vitro and in vivo degradation of films of chitin and its deacetylated derivatives. Biomaterials 18: 567–575.
7. Abdou ES, Nagy KS, Elsabee MZ (2008) Extraction and characterization of chitin and chitosan from local sources. Bioresour Technol 99: 1359–1367.
8. Dutta PK, Dutta J, Tripathi VS (2004) Chitin and chitosan? Chemistry, properties and applications. J Sci Ind Res 63: 20–31.
9. Cai J, Yang J, Du Y, Fan L, Qiu Y, et al. (2006) Enzymatic preparation of chitosan from the waste *Aspergillus niger* mycelium of citric acid production plant. Carbohydr. Polym 64: 151–157.
10. Parada LG, Miranda R, Salvador S (2004) Caracterización de quitosano por viscosimetría capilar y valoración potenciométrica. Rev Iberoam polímeros 5: 1–16.
11. Dos Santos ZM, Caroni AL, Pereira MR, da Silva DR, Fonseca JL (2009) Determination of deacetylation degree of chitosan: a comparison between conductometric titration and CHN elemental analysis. Carbohydr Res 344: 2591–2595.
12. Baxter S, Zivanovic S, Weiss J (2005) Molecular weight and degree of acetylation of high-intensity ultrasonicated chitosan. Food Hydrocoll 19: 821–830.
13. VandeVord PJ, Matthew HW, DeSilva SP, Mayton L, Wu B, et al. (2002) Evaluation of the biocompatibility of a chitosan scaffold in mice. J Biomed Mater Res 59: 585–590.
14. Sachlos E, Czernuszka JT (2003) Making tissue engineering scaffolds work. Review: the application of solid freeform fabrication technology to the production of tissue engineering scaffolds. Eur Cell Mater 5: 29–39.
15. Chen X, Liu CS, Liu CG, Meng XH, Lee CM, et al. (2006) Preparation and biocompatibility of chitosan microcarriers as biomaterial. Biochem. Eng J 27: 269–274.
16. Zhuang PY, Li YL, Fan L, Lin J, Hu QL (2012) Modification of chitosan membrane with poly(vinyl alcohol) and biocompatibility evaluation. Int J Biol Macromol 50: 658–663.
17. Huang H, Lin W, Lin J (2004) Chitosan Obtained from Cell Wall of *Aspergillus Niger* Mycelium. Chem Res Chinese Univ 20: 156–158.
18. Muñoz G, Valencia C, Valderruten N, Ruiz-Durántez E, Zuluaga F (2015) Extraction of chitosan from *Aspergillus niger* mycelium and synthesis of hydrogels for controlled release of betahistine. React Funct Polym 91–92.
19. Kasaai MR, Arul J, Charlet G (2000) Intrinsic viscosity-molecular weight relationship for chitosan. J. Polym. Sci Part B Polym Phys 38: 2591–2598.
20. Fernandez-Megia E, Novoa-Carballeda R, Quiñoá E, Riguera R (2005) Optimal routine conditions for the determination of the degree of acetylation of chitosan by ¹H-NMR. Carbohydr Polym 61: 155–161.
21. Kasaai MR (2010) Determination of the degree of N-acetylation for chitin and chitosan by various NMR spectroscopy techniques: A review. Carbohydr Polym 79: 801–810.
22. Kasaai MR (2007) Calculation of Mark–Houwink–Sakurada (MHS) equation viscometric constants for chitosan in any solvent–temperature system using experimental reported viscometric constants data. Carbohydr Polym 68: 477–488.
23. (2011) ASTM International. Standard Test Method for in vitro Degradation Testing of Hydrolytically Degradable Polymer Resins and Fabricated Forms for Surgical Implants (F1635-11) 1–7.
24. (2010) ASTM International. Standard Test Method for Tensile Properties of Plastics (D638-10) 1–16.
25. Cárdenas G, Anaya P, von Plessing C, Rojas C, Sepúlveda J (2008) Chitosan composite films. Biomedical applications. J Mater Sci Mater Med 19: 2397–2405.

26. Leceta I, Guerrero P, de la Caba K (2013) Functional properties of chitosan-based films. Carbohydr Polym 93: 339-346.
27. (2009) International Standard Organization. Biological evaluation of medical devices - Part 6: tests for local effects after implantation (ISO 10993) 6: 1-38.
28. Gartner C, López BL, Sierra L, Graf R, Spiess HW, et al. (2011) Interplay between structure and dynamics in chitosan films investigated with solid-state NMR, dynamic mechanical analysis, and X-ray diffraction. Biomacromolecules 12: 1380-1386.
29. Nwe N, Furuike T, Tamura H (2012) Production of Fungal Chitosan by Enzymatic Method and Applications in Plant Tissue Culture and Tissue Engineering? 11 Years of Our Progress, Present Situation and Future Prospects; Intech: Rijeka, Croatia.
30. White SA, Farina PR, Fulton I (1979) Production and isolation of chitosan from *Mucor rouxii*. Appl Environ Microbiol 38: 323-328.
31. Miyoshi H, Shimura K, Watanabe K, Onodera K (1992) Characterization of some fungal chitosans. Biosci Biotechnol Biochem 56: 1901-1905.
32. Cundumí N, Arango J (1994) Diseño del proceso de obtención de Quitosana a partir de Micelio, subproducto en la síntesis de Acido Citrico, Tesis de Pregrado (Ingeniería Química). Universidad del Valle. Facultad de Ingeniería. Escuela de Ingeniería Química.
33. Díaz Bojorge DA (2010) Actividad antifúngica del quitosano sobre semillas de maíz (*Zea mays*) afectadas por el hongo *Fusarium oxysporum*, Tesis de Pregrado (Química). Universidad del Valle. Facultad de Ciencias Naturales y Exactas. Departamento de Química.
34. Muñoz GA (2012) Obtención de hidrogeles de quitosano a partir del micelio de *Aspergillus niger* para la liberación controlada de fármacos, Tesis de Maestría (Química). Universidad del Valle. Facultad de Ciencias Naturales y Exactas, Departamento de Química.
35. Kumirska J, Czerwicka M, Kaczynski Z, Bychowska A, Brzozowski K, et al. (2010) Application of spectroscopic methods for structural analysis of chitin and chitosan. Mar Drugs 8: 1567-1636.
36. Pawlak A, Mucha M (2003) Thermogravimetric and FTIR studies of chitosan blends. Thermochim. Acta 396, 153-166.
37. Abdel-Fattah WI, Jiang T, El-Bassyouni Gel-T, Laurencin CT (2007) Synthesis, characterization of chitosans and fabrication of sintered chitosan microsphere matrices for bone tissue engineering. Acta Biomater 3: 503-514.
38. Neto CGT, Giacometti JA, Job AE, Ferreira FC, Fonseca JLC, et al. (2005) Thermal Analysis of Chitosan Based Networks. Carbohydr. Polym 62: 97-103.
39. Zhang Y, Xue C, Xue Y, Gao R, Zhang X (2005) Determination of the degree of deacetylation of chitin and chitosan by X-ray powder diffraction. Carbohydr Res 340: 1914-1917.
40. Suyatma NE, Tighzert L, Copinet A, Coma V (2005) Effects of hydrophilic plasticizers on mechanical, thermal, and surface properties of chitosan films. J Agric Food Chem 53: 3950-3957.
41. Azad AK, Sermisintham N, Chandkrachang S, Stevens WF (2004) Chitosan membrane as a wound-healing dressing: characterization and clinical application. J Biomed Mater Res B Appl Biomater 69: 216-222.
42. Van Vlierberghe S, Dubruel P, Schacht E (2011) Biopolymer-based hydrogels as scaffolds for tissue engineering applications: a review. Biomacromolecules 12: 1387-1408.
43. Sánchez A, Sibaja M, Vega-Baudrit J, Madrigal S (2007) Síntesis y caracterización de hidrogeles de quitosano obtenido a partir del camarón langostino (*Pleuroncodes planipes*) con potenciales aplicaciones biomédicas. Rev Iberoam. Polímeros 8: 241-267.
44. Nwe N, Furuike T, Tamura H (2009) The Mechanical and Biological Properties of Chitosan Scaffolds for Tissue Regeneration Templates Are Significantly Enhanced by Chitosan from *Gongronella butleri*. Materials 2: 374-398.
45. Hilmi AB, Halim AS, Hassan A, Lim CK, Noorsal K, et al. (2013) In vitro characterization of a chitosan skin regenerating template as a scaffold for cells cultivation. Springerplus 2: 79.
46. Murphy CM, Haugh MG, O'Brien FJ (2010) The effect of mean pore size on cell attachment, proliferation and migration in collagen-glycosaminoglycan scaffolds for bone tissue engineering. Biomaterials 31: 461-466.
47. Hollister S (2006) Porous scaffold design for tissue engineering. Nat Mater 5: 590.
48. Batchelor A, Chandrasekaran M (2004) Service Characteristics Of Biomedical Materials And Implants. Imperial College Press.
49. Hurt AP, Getti G, Coleman NJ (2014) Bioactivity and biocompatibility of a chitosan-tobermorite composite membrane for guided tissue regeneration. Int J Biol Macromol 64: 11-16.
50. Algul D, Sipahi H, Aydin A, Kelleci F, Ozdatli S, et al. (2015) Biocompatibility of biomimetic multilayered alginate-chitosan/ β -TCP scaffold for osteochondral tissue. Int J Biol Macromol 79: 363-369.
51. Martel-Estrada SA, Rodríguez-Espinoza B, Santos-Rodríguez E, Jiménez-Vega F, García-Casillas PE, et al. (2015) Biocompatibility of chitosan/*Mimosa tenuiflora* scaffolds for tissue engineering. J Alloys Compd 643: S119-S123.
52. Brito MK, Schellini SA, Padovani CR, Pellizzon CH, Trindade-Neto CG (2009) [Chitosan inclusions in the subcutaneous space of rats: clinic, histologic and morphometric evaluation]. An Bras Dermatol 84: 35-40.
53. Dash M, Chiellini F, Ottenbrite RM, Chiellini E (2011) Chitosan - A versatile semi-synthetic polymer in biomedical applications. Prog Polym Sci 36: 981-1014.
54. Boot RG, Renkema GH, Strijland A, van Zonneveld AJ, Aerts JM (1995) Cloning of a cDNA encoding chitotriosidase, a human chitinase produced by macrophages. J Biol Chem 270: 26252-26256.